Key Engineering Materials Vols. 326-328 (2006) pp. 277-280
online at http://www.scientific.net

Correlation between Microstructure and Nanohardness in Advanced Heat-Resistant Steel

Jae-il Jang[1, a], Sanghoon Shim[2, 3, b], Shin-ichi Komazaki[4, c], and Takayuki Sugimoto[5, d]

[1]Div. of Mater. Sci. & Eng., Hanyang University, Seoul 133-791, Korea

[2]Dept. of Mater. Sci. & Eng., The University of Tennessee, Knoxville, TN 37996-2200, USA

[3]Metals & Ceramics Div., Oak Ridge National Laboratory. Oak Ridge, TN 37831, USA

[4]Dept. of Mater. Sci. & Eng., Muroran Institute of Technology. Muroran 050-8585, Japan

[5]Nikko Inspection Service Co. Ltd., Muroran 051-8505, Japan

[a] jijang@hanyang.ac.kr, [b] shims@ornl.gov, [c] komazaki@mmm.muroran-it.ac.jp,

[d] takayuki_sugimoto@jsw.co.jp

Keywords: Nanoindentation, Heat-resistant steel, Lath-martensitic structure, Strengthening Mechanism.

Abstract. As advanced ferritic/martensitic heat-resistant steels generally have a complex structure consisting of several microstructural units (lath, block, packet, and prior austenite grain), it is very hard to separate the contribution of each microstructural unit (or its each boundary) to the strengthening mechanism in such steels. Here we explore the role of each microstructural unit in strengthening of advanced high Cr steel through nanoindentation experiments performed at different load levels. Nanoindentation results are analyzed by comparing with microstructural observations and discussed in terms of prevailing descriptions of strengthening mechanism.

Introduction

Recently, advanced 9-12% Cr martensitic/ferritic steels (e.g. P92 for 9%Cr steel and P122 for 12%Cr steel) have received attentions as strong candidates as materials for ultra-super-critical (USC) boilers because of better high temperature strength as well as oxidation- and corrosion-resistance than those of conventional 9-12% Cr steels. It is known that the excellent strength performances of these steels are due to the combined strengthening mechanisms of the matrix and grain boundaries. As the ferritic/martensitic heat-resistant steels generally have a complex lath-martensitic structure consisting of several microstructural units (i.e., in the order of their size, (1) extremely fine lath, (2) block and/or packet including several laths, and (3) prior austenite grain which is the largest unit), it is very hard to separate the contribution of each microstructural unit (i.e., each grain boundary) to the strengthening mechanism in the steels. So, for better and more systematic understanding of the role of each microstructural unit, some novel techniques to measure localized strength are essential. One possible way to directly measure individual strength characteristics of complex microstructures with sub-micron dimensions is nanoindentation, which can evaluate the nanohardness of localized region solely using indentation load-depth curves without measurement of the permanent residual indents [1]. Very recently, some pioneering works in applying the nanoindentation technique to strength analysis of martensitic steels were performed by Ohmura et al. [2,3], who suggested that matrix strength of Fe-C binary martensitic steels can be successfully measured by nanoindentation (performed mainly at 0.5 mN) without contribution of high-angle boundaries (such as block, packet, and prior austenite grain boundaries). With this in mind, we explored the role of each microstructural unit and its boundary in strengthening of modified 12% Cr steel (recently developed for the application to steam turbine rotor for the USC boiler) through nanoindentation experiments together with microstructural analysis.

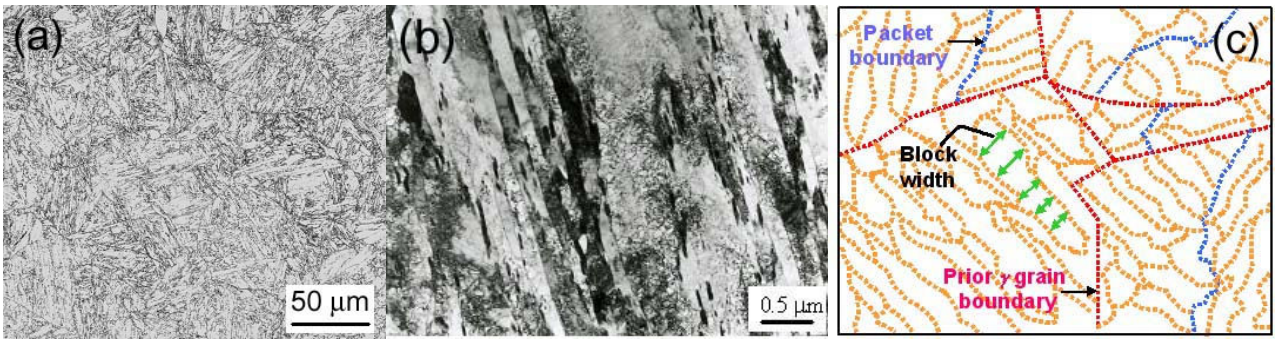

Fig.1. Examples of microstructural observations; (a) OM image, (b) TEM image, and (c) grain boundary map to measure the block width.

Experimental Details

The material used in this study is a modified 12%Cr ferritic steel whose chemical composition except for Fe is 10.02Cr-0.99Mo-0.19V-1.00W-0.14C-0.05Nb-0.0373N-0.04Si-0.62Mn-0.007P-0.0025S-0.70Ni as mass%. The steel was normalized and tempered under typical heat-treatment conditions for turbine rotors. The microstructural features were examined by optical microscopy (OM) and transmission electron microscopy (TEM). The TEM observations were carried out using a JEM-200CX (Japan Electron Microscope, Japan) at 200 kV.

Nanoindentations were performed using a Nanoindenter-XP (MTS Corp., Oak Ridge, TN) with a typical Berkovich indenter tip. Maximum indentation load (Pmax) was varied (0.5, 1, 5, 10, 50, 100, 400, and 700 mN) while loading/unloading rate was fixed as (Pmax/50) mN/sec to obtain sufficient data points. No rate effect was observed. The calibration and calculation of nanohardness was conducted by the Oliver-Pharr method [1]. All data were obtained from electro-polished samples instead of mechanically-polished samples, in order to avoid mechanical-polishing-induced hardening effects. The specimen surface was electrically polished in a phosphoric-acid-solution (100 ml)-added chromium oxide (VI) (50 g) at a temperature of 348 K and under current density of 0.8 mA/mm^2 for 60 s after grinding and mechanical polishing.

Results and Discussion

Figures 1(a) and 1(b) shows a representative OM and TEM images of the tested material. The sample exhibited a typical tempered lath martensitic structure without any delta ferrite. The microstructure consists of lath martensite containing a high density of dislocations in the lath interior, which was produced by the martensitic transformation during normalizing. The OM and TEM images revealed the size of prior austenite grain (i.e., the biggest microsturural unit of this material) and width of lath martensite (i.e., the smallest one) respectively; the former is larger than 50 μm, and the latter is around 0.2~0.5 μm, which is in relatively good agreement with the value reported elsewhere [4]. It was more difficult to determine the size of block than measuring the sizes of lath and prior austenite grain, and unfortunately we could not critically judge the boundary of packet in this study. To determine the block width, we performed more severe etching than used for Fig. 1(a), and measured the widths of more than 30 blocks by the way of grain boundary mapping (see Fig. 1(c)). As a result, the averaged block width was found to be approximately 2 ~ 3 μm, which is well agreed with the value recently reported by Kimura et al. [5].

Figure 2(a) shows the results from nanoindentation experiments performed at different indentation load levels. The nanoindentation hardness values extracted from indentation curve (through Oliver-Pharr method [1]) were plotted as a function of maximum indentation load. Interestingly, the tendency of hardness variation with Pmax can be roughly divided into two groups, i.e. relatively high load region (Pmax ≥ 10 mN) and low-load region (Pmax ≤ 10 mN). In high load region, hardness decreases with increasing indentation load, which seems to be explained by the

well-known 'the smaller, the harder' concept of indentation size effect (ISE) (see the review article [6]). To check out the possible extension of this tendency, we carried out Vickers hardness tests at a load of 9.8 N, and obtained the hardness value of about 3.2 ~ 3.3 GPa without large data scatter. Note that this Vickers hardness was obtained based on 'projected area' of the indentation instead of 'surface area' (generally used for Vickers hardness measurement), in order to directly compare with nanoindentation hardness. Since obtained Vickers hardness is smaller than nanoindentation hardness measured at the highest load of 700 mN, it is reasonable to believe that the tendency of hardness decrease with increasing load continues at higher loads.

On the other hand, it was observed in low load region (Pmax ≤ 10 mN) that nanohardness increases as the applied load increases. This is curious since this tendency is directly opposite to the concept of indentation size effect (ISE) [6]. This inverse-ISE behavior might be explained by complex nature of lath martensitic microstructure in this steel. Although precise quantification cannot be achieved, some insight can be gained by comparing the size of each microstructure unit and the plastic zone size under the indenter. According to the Johnson's expanding cavity model for elastic-plastic indentation with a cone [7], the ratio of plastic zone radius (b) to contact radius (a) can be given as:

$$\frac{\mathbf{b}}{\mathbf{a}} = \{\frac{1}{6(1-\boldsymbol{\nu})}[\frac{\mathbf{E}}{\boldsymbol{\sigma}_{\mathbf{YS}}}\tan\boldsymbol{\beta} + 4(1-2\boldsymbol{\nu})]\}^{1/3} \quad (1)$$

where β is the angle of inclination of the indenter to the surface of the edge of indentation, E is Young's modulus, ν is Poisson's ratio, and σ_{YS} is the yield strength. Therefore, if information about material properties and indenter geometry is provided, the ratio of (b/a) can be determined as a constant. In order to relate this conical indentation model to the results obtained here, it is useful to make the normal assumption that similar behavior is obtained when the angle of the cone gives the same area-to-depth relation as the pyramid. For the Berkovich indenter (whose centerline-to-face angle is 65.3°), the equivalent cone angle is 70.3° and thus β is 19.7°. Accordingly, by putting E = 200 GPa, σ_{YS} = 710 MPa (obtained from standard tensile tests [8]), ν = 0.3 and β = 19.7° into the right side of Eq. 1, and then the contact radii at various maximum loads (which were determined by Oliver-Pharr method [1]) into the left term of the equation, we could estimate the plastic zone size under the indenter. The average values of the estimated plastic zone sizes were approximately 0.6 μm for Pmax = 0.5 mN, 0.8 μm for 1 mN, 1.8 μm for 5 mN, 2.5 μm for 10 mN, 5.6 μm for 50 mN, 8.2 μm for 100 mN, 16.6 μm for 400 mN, and 22.5 μm for 700 mN respectively. Note that the shape of the plastic zone is assumed as a hemi sphere according to Johnson's model [7].

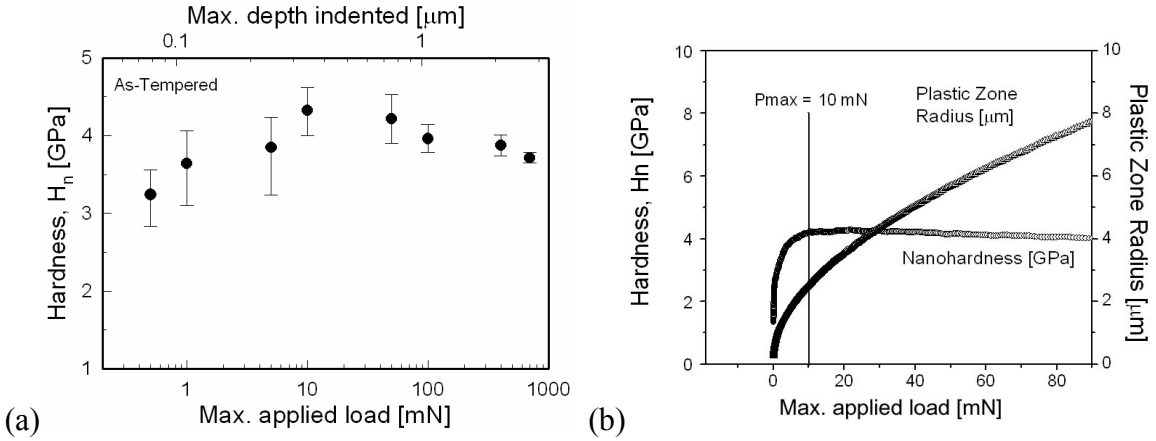

Fig. 2. Results from nanoindentation experiments; (a) variation in nanohardness with increasing applied indentation load (and depth), and (b) a CSM result showing the variations in both hardness and plastic zone radius according to the change in the indentation load.

At Pmax = 0.5 mN, the calculated 'diameter' of hemi-spherical plastic zone is around 1.2 μm, which is larger than the lath width, but smaller than the averaged block width. Therefore, at such a low load, it is possible that the material under the indenter includes only lath boundaries. Since a lath boundary is known to be a low angle boundary, one might consider that the block (or packet) is essentially a single crystal of martensite [9]. Thus, it seems reasonable to assume that the obtained hardness is the matrix strength of this steel. At Pmax = 1 mN, the diameter of plastic zone (about 1.6 μm) is still a little smaller than the average block width (2 ~ 3 μm). However, the possibility for the material under indenter to have a block boundary within its plastic zone is bigger than that at Pmax = 0.5 mN. So, hardness can increase due to the possible block boundary strengthening effect. At Pmax = 5 mN, plastic zone diameter is about 3.6 μm, and the material under the indenter should meet one or two block boundaries and thus the influences of block boundary strengthening (and resultantly hardness value) are bigger than those at Pmax = 1 mN. When indentation peak load increases up to 10 mN, the plastic zone diameter is around 5.0 μm. Although this size is still much smaller than prior austenite grain size, it might be large enough to have significant block boundary effects. In higher load region (Pmax > 10mN), hardness decreases with increasing load level, even though the plastic zone sizes are much larger than that at P max = 10mN. The same tendency was also clearly observed during continuous hardness measurement performed using 'continuous stiffness measurement' (CSM) technique [1], as shown in Fig. 2(b). Note that the principle of 'the smaller, the harder' (i.e., ISE) works only if there is no significant change in microstructural environment sampled. So, above results may imply that (1) both the 10 mN and 700mN indentations have a similar microstructural environment despite the different size, and thus (2) plastic zone size for Pmax = 10mN is already big enough to reflect the block boundary effect. Based on all above results, it is possible to conclude that packet boundaries (since the packet is a bigger microstructure unit than the block) and prior austenite grain are not so effective in strengthening the this material and thus that, with a viewpoint of grain boundary strengthening, the block size is indeed effective grain size of this steel, i.e., macroscopic strength of this steel is certainly enhanced by the block boundaries rather than other high angle boundaries (such as packet and prior austenite grain boundary).

Conclusion

Influence of microstructures on strengthening mechanism in advanced 12%Cr ferritic steel was investigated using nanoindentation experiments. Results presented here show that block boundary is more effective for enhancing strength than other high angle boundaries in this steel. To completely understand the deformation behavior of this steel, analysis of yielding behavior (possibly through pop-in analysis of spherical/blunted tip nanoindenation) seems to be additionally desirable.

Acknowledgement

This work was supported by the research fund of Hanyang University (HY-2005-000-0000-1266).

References

[1] W.C. Oliver and G.M. Pharr: J. Mater. Res. Vol. 7 (1992), p. 1564.
[2] T. Ohmura, K. Tsuzaki and S. Matsuoka: Scripta Mater. Vol. 45 (2001), p. 889.
[3] T. Ohmura, T. Hara and K. Tsuzaki: J. Mater. Res. Vol. 18 (2003), p. 1465.
[4] R. Ishii, Y. Tsuda, K. Fujiyama, K. Kimura et al.: Tetsu-to-Hagane, Vol. 89 (2003), p. 699.
[5] M. Kimura, K. Yamaguchi, M. Hayakawa et al.: Tetsu-to-Hagane, Vol. 90 (2004), p. 27.
[6] H. Gao and Y. Huang: Scripta Mater. Vol. 48 (2003), p. 113.
[7] K.L. Johnson: J. Mech. Phys. Solids Vol. 18 (1970), p. 115.
[8] M. Yamada, O. Watanabe, Y. Yoshioka et al.: Tetsu-to-Hagane, Vol.76 (1990), p. 1084.
[9] J.W. Morris, Jr., Z. Guo, C.R. Krenn and Y.-H. Kim: ISIJ Int., Vol. 41 (2001), p. 599.